

Ballute Aerocapture Trajectories at Titan

Daniel T. Lyons
Wyatt Johnson

Jet Propulsion Laboratory
California Institute of Technology
Pasadena, CA 91109

daniel.t.lyons@jpl.nasa.gov

(818) 393-1004
(818) 393-9900 (FAX)

Abstract:

Aerocapture at planets and moons with atmospheres using a towed, inflatable ballute system has the potential to provide significant performance benefits compared to traditional all propulsive and aeroshell based aerocapture technologies. This paper discusses the characteristics of entry trajectories for ballute aerocapture at Titan. These trajectories are the first steps in a larger systems analysis effort that is underway to characterize and optimize the performance of a ballute aerocapture system for future missions to Titan.

Introduction:

A "Ballute" is a cross between a "balloon" and a "Parachute". The inflated components provide the stiffness needed to maintain the proper shape of a very light weight structure, while the large drag area acts like a parachute to slow the spacecraft rapidly once it enters the upper atmosphere of the target body. Preliminary studies of ballutes for aerocapture at several planetary bodies were pioneered by Angus McRonald.^{1,2,3} Jeff Hall has also made recent contributions to the advancement of ballute technology⁴. More recently, an interdisciplinary team of engineers lead by Kevin Miller (Ball Aerospace) is starting to take a closer look at characterizing and refining the use of ballutes for future aerocapture missions^{5,6}. The team includes experts from Ball Aerospace (system engineering), ILC Dover (inflatable structures), NASA Langley Research Center (aerothermodynamics and hypersonic performance verification), and the Jet Propulsion Laboratory (trajectories, mission design, and instrumentation). Preliminary calculations have shown that Titan aerocapture ballutes could be constructed using existing materials. These large, lightweight inflatable structures would provide a significant mass savings over traditional all-propulsive vehicles or aerocapture using a heat shield, especially when a special transfer

stage is required to provide power and attitude control during cruise. In addition to the low additional mass of the ballute for aerocapture, one of the fundamental benefits of carrying a ballute is that the primary spacecraft bus does not have to remain tightly packed for cruise, but can be deployed and flown like an orbiter.

All propulsive capture requires that the spacecraft must carry all of the propellant needed for the mission. For low altitude orbiters, the mass of the propellant for a traditional all propulsive spacecraft becomes so large that the useful science payload becomes too small to be cost effective. In some cases, such as missions to Titan and Neptune, it may not be possible to conduct an orbital mission without aerocapture and/or other advanced propulsion technologies. One alternative for reducing the amount of propellant that must be carried is to use atmospheric drag to provide the velocity change required to capture into orbit.

Ballute Aerocapture: High Drag, Low Heating

The traditional approach is to pack the spacecraft tightly inside a protective aeroshell and dive deep into the atmosphere, where the heat shield must provide protection against the extremely large heating rates that will be encountered. Everyone associated with the space program is so familiar with the high heating rates associated with this traditional atmospheric entry technique, that it would be easy to make the mistake of assuming that high heating is an unavoidable fact of life for all forms of aerocapture. High heating is not required for aerocapture when a large ballute is used to supply the drag.

Rather than diving deep into the atmosphere to get enough drag to aerocapture, imagine instead the approach used for aerobraking, where the spacecraft is so high in the atmosphere that the heating rate is tolerable even for an unprotected spacecraft. As the area of such a spacecraft is increased, the amount of drag force on the spacecraft increases, but the heating per unit area remains relatively constant. The ballute concept takes this idea to the limit by dramatically increasing the area of the spacecraft so that enough drag is produced to remove the energy required to capture into orbit in a single pass through the atmosphere. Assuming that the entry velocity is determined by the interplanetary trajectory, the heating rate is primarily a function of the atmospheric density, but the drag force is a function of both the density and the projected frontal area. The ballute system can be designed so that an unprotected spacecraft could survive the aerocapture heating rates if the drag producing area is made large enough. Smaller ballutes require higher heating rates, because they have to fly deeper in the atmosphere, but they also weigh less because they require less material. These smaller ballutes require some thermal protection for the spacecraft because a kapton ballute can survive at 500°C, whereas most spacecraft components cannot. Most of the ballute concepts studied by our team have been for heating rates that can be accommodated by the thin kapton film of the ballute, rather than the heating rates

that can be accommodated by most unprotected spacecraft. Since kapton can survive higher temperatures than most spacecraft components, using the kapton thermal limits as the system limit means that the main spacecraft bus must be protected by a lightweight thermal blanket on the side facing into the "wind". The ultimate trade between the weight of the blanket and the weight (and size) of the ballute is made at the system level to assure that the maximum spacecraft payload will be safely captured into orbit.

The Ballute Aerocapture Trajectory Corridor:

The trajectory component of our team effort will be described in this paper. A typical ballute aerocapture trajectory begins as a hyperbolic approach trajectory which would fly past the planet if there were no atmosphere. The ballute is deployed and inflated hours before entry with the aerodynamically stable axis of the spacecraft/ballute system aligned with the velocity near entry. Upon entering the atmosphere, the spacecraft experiences a large deceleration that usually reaches a maximum value before the spacecraft reaches periapsis. The deceleration eventually decreases as the velocity slows down, even though the atmospheric density may still be increasing. When the desired separation condition is reached, the spacecraft must release the ballute to minimize further velocity loss due to drag. Releasing the ballute at precisely the right moment is critical to minimizing the propellant required to ultimately achieve the desired final orbit. Since the deceleration at the time of release is usually large, the ballute must be released within about one second of the optimum time to achieve an acceptable total change in velocity. Separation mechanisms have been flown with timing uncertainties of about 10 milliseconds, so a 0.5 sec timing requirement for the release mechanism is not a showstopper.

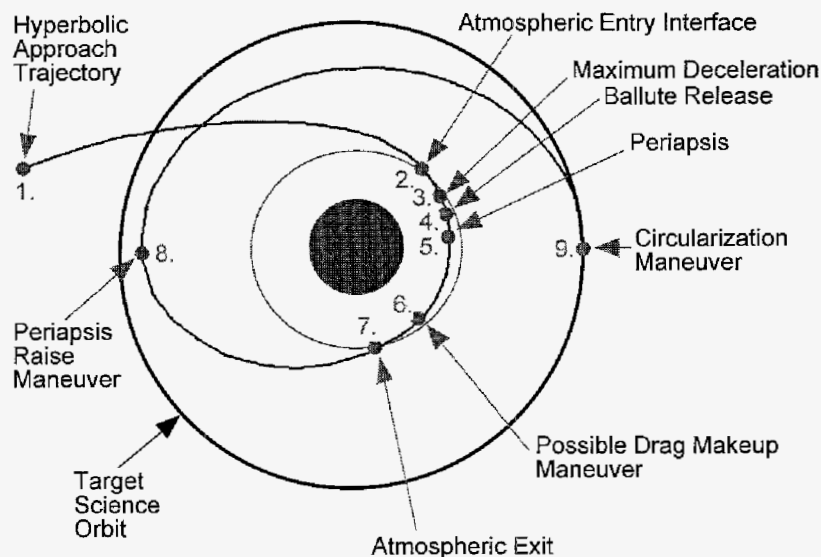


Figure 1: Sequence of Events along a Ballute Aerocapture Trajectory

In the perfect universe of our computer simulations, the heating during ballute aerocapture for a particular vehicle design is minimized if the periapsis altitude of the approach hyperbola is so high in the atmosphere that the target apoapsis is not achieved until the moment that the spacecraft leaves the atmosphere. Such a trajectory would "barely" achieve the target orbit by holding on to the ballute for the entire duration of the drag pass. In the real world, a very small navigation error which put the actual periapsis altitude a little higher than expected, or an atmosphere that was slightly less dense than expected would mean that there would not be enough drag to achieve the desired orbit apoapsis. A slightly larger error could mean that the spacecraft might not even be captured into orbit, but would leave on a slower hyperbolic orbit than the one it arrived on. A ballute system can accommodate these uncertainties in navigation, drag-coefficient, and average atmospheric density by aiming the approach hyperbola lower in the atmosphere than required to barely capture and then releasing the ballute earlier in the drag pass, once enough delta-V had been achieved. Larger atmospheric and navigation uncertainties require targeting the nominal trajectory deeper into the atmosphere. Unfortunately, targeting the nominal trajectory deeper results in higher deceleration loads, higher heating rates, and more uncertainty in the orbital state at exit from the atmosphere. Thus, the nominal target must be carefully balanced between the conflicting requirements to maximize the probability of capturing while minimizing the propellant required to ultimately circularize the orbit.

Although the aeroshell community uses Entry Flight Path Angle to define the range of acceptable entry conditions, the periapsis radius of the approach hyperbola was used for this study because it is independent of the entry radius. There are two limits to the periapsis radius of the approach hyperbolic trajectories that can achieve the desired target apoapsis. The upper limit assumes that the spacecraft barely achieves the desired apoapsis altitude at exit if the ballute is never released, as described earlier. The lower limit requires releasing the ballute as soon as the spacecraft enters the atmosphere. If the drag from the spacecraft alone is enough to achieve the target orbit, approaching on a lower altitude hyperbola will result in too much drag. Although such lower altitude limit trajectories can be found in the perfect universe of the computer simulation, they don't use the ballute to produce drag, and are equivalent to a ballistic capture by the spacecraft alone. Thus the lower trajectory limit would require the heavy heat shield that the ballute system is trying to avoid. A trajectory that approached on this lower limit would have no ability to target the desired apoapsis by choosing the time of release, because the drag occurs after release. In between these two high and low altitude extremes is a relatively wide corridor of possible trajectories that can be used to accommodate relatively large uncertainties in approach navigation and atmospheric density.

Choosing the Targeted Trajectory:

As the aim point is targeted deeper into the atmosphere, the ballute must be released earlier in order to achieve a specific apoapsis altitude target at exit from the atmosphere. An earlier ballute release means that there is more time for drag to change the velocity of the spacecraft after release, and it implies that the drag effects on the spacecraft after release will be larger and therefore harder to predict. Atmospheric uncertainty before the ballute release can be accommodated by monitoring the actual deceleration of the vehicle, and then modifying the release time. Once the ballute is released, however, the primary way to accommodate the effects of atmospheric uncertainty on the remainder of the trajectory is to use propellant to correct the trajectory later in the orbit. The amount of drag experienced after separation can be reduced by using a larger, but more massive ballute to reduce the density and thus reduce the drag experienced after separation. The absolute magnitude of the density after separation is less for a larger ballute, because the nominal trajectory is targeted higher in the atmosphere. Thus there is an implicit tradeoff between the mass of the ballute and the mass of propellant required to achieve the final orbit. A balanced system design will require targeting the ballute system low enough to provide adequate margins to accommodate atmospheric and navigation uncertainties, but high enough to minimize the propellant that must be carried to remove the targeting errors. Since at least one propulsive maneuver is required to raise periapsis out of the atmosphere, the question that must be answered is how much additional propellant is required to accommodate the probable dispersion in the ballute trajectory at atmospheric exit ?

Atmospheric and Navigation Uncertainties:

The ballute aerocapture task at Titan has been able to leverage off the work for a similar aerocapture task that was started about a year earlier than the Titan ballute task by an interdisciplinary team from several NASA Centers. That task assumed that the spacecraft would be a lifting aeroshell. They developed not only a very detailed atmosphere model for Titan⁷, but it also provided a reference mission, including a dispersed set of 2000 entry states⁸. In order to provide a meaningful comparison between ballutes and aeroshells, our team has been evaluating the performance of ballutes for the same reference mission used as the basis for the aeroshell study. The mission timeline from the aeroshell study is shown in Figure 2, where the events between entry and exit from the atmosphere have been updated for a ballute mission.

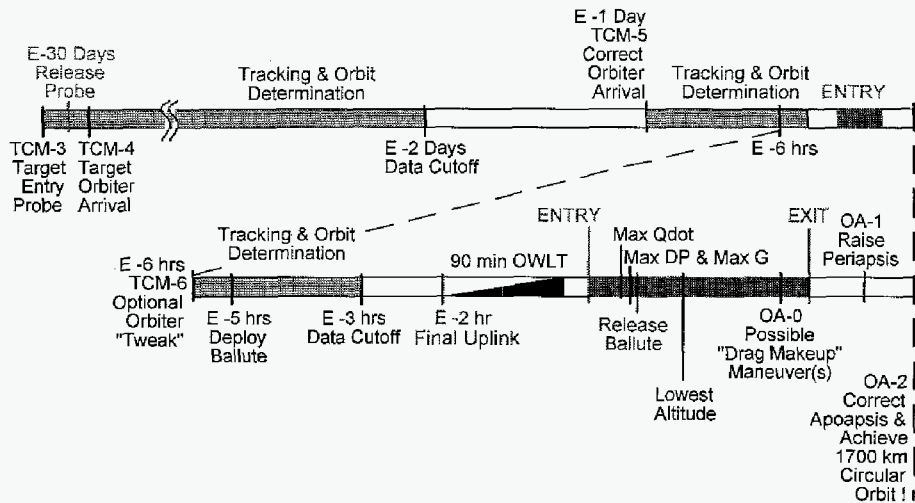


Figure 2: Timeline of Events

The Titan aeroshell reference mission⁹ was based on the results of a trade study that showed that a Solar Electric Propelled spacecraft with a Venus gravity assist could deliver a reasonable payload to Titan in a reasonable time (a 7 year cruise). It assumed that the approaching spacecraft would release an entry probe 30 days before arrival, and would then retarget the main spacecraft on an aerocapture entry trajectory. Two sets of 2001 entry states were computed to represent the “delivery” and “knowledge” capabilities of a spacecraft using typical performance characteristics for Doppler, range, optical, and Δ DOR navigation data types. Tracking data for the “delivery” uncertainties was assumed to end 2 days prior to entry, whereas data for the “knowledge” uncertainties was assumed to end 3 hours before entry. The 3 hour cutoff was selected to allow time for the Nav Team to process the data on the ground and then upload an updated set of parameters to the spacecraft before entry. The timeline also included a final targeting maneuver 1 day before entry, and a placeholder for a last minute trajectory correction 6 hours before entry. The entry trajectory was targeted to arrive at Titan with an entry speed of 6.5 km/sec, which was representative of a 7 year interplanetary cruise. The entry flight path angle for the aeroshell mission was -37° . The most important uncertainty for the entry state was the entry flight path angle, which had 1-sigma dispersion of 0.30° for the “delivery” assumptions, and a 1-sigma dispersion of 0.06° for the “knowledge” assumptions. The uncertainty in the entry speed was negligible - only 0.01 m/s! These values assumed that the ephemeris of Titan would be updated based on a successful Cassini Mission.

Figure 3 shows the scatter in the osculating periapsis altitude of the approach hyperbola for the nominal and 2000 entry trajectories that were dispersed to simulate “knowledge” uncertainties. In order to retarget the aeroshell trajectories to the higher periapsis altitude (shallower entry flight path angle) required by the ballute system, the V_∞ vector, inclination, and node of the original states were held constant for each trajectory while the approach

periapsis radius was increased by the same amount for all of the trajectories. The amount of increase was determined by searching for the value where the highest altitude trajectory would barely achieve the desired apoapsis altitude at exit when the thinnest possible atmosphere model was used. Choosing the nominal radius of periapsis target using this procedure guarantees that it is possible to find a release time that will achieve the desired osculating apoapsis altitude at exit for all possible combinations of atmosphere models and adjusted “knowledge” entry states.

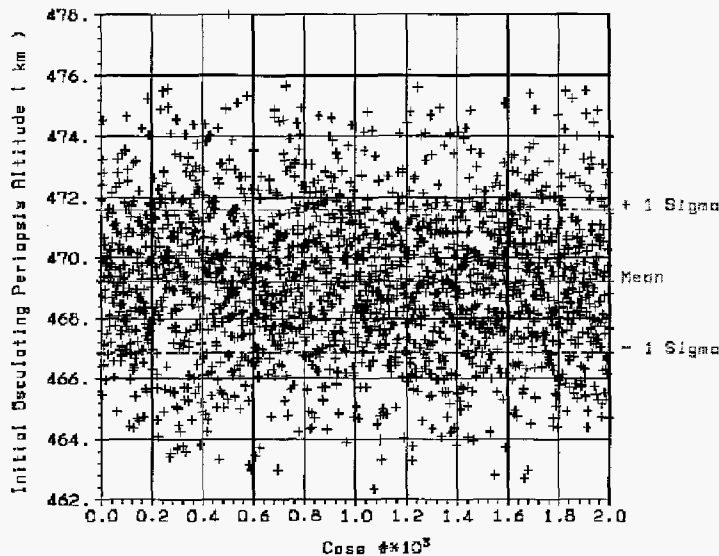


Figure 3: Dispersed Periapsis Altitudes for the 2001 Retargeted Approach Hyperbolas (Knowledge assumptions)

Guaranteeing that a release time exists which achieves the target may not be the best way to pick the target periapsis radius. For example, for this set of 2000 perturbed states, the highest altitude case which was used to determine the target is an extremely unlikely value – being about 4-sigma from the mean (as shown in Figure 3). Furthermore, the probability that the atmosphere is the “thinnest possible” that can be obtained from TitanGRAM is also extremely unlikely, since the F_{minmax} parameter was meant to span all possible conditions, including seasonal and latitudinal effects. As will be shown later, accommodating such a broad range of atmospheric densities, although possible, leads to undesirable performance for densities that are not much greater than the “average”.

The density profiles used in the simulations were obtained by querying TitanGRAM with different values of the “ F_{minmax} ” parameter. An F_{minmax} of 0 is meant to represent an average density profile. An F_{minmax} of 1 represents the highest density profile, while an F_{minmax} of -1 represents the thinnest density profile. There are no latitudinal, seasonal, or diurnal effects in the current beta version of TitanGRAM. The extremes of these parameters are all lumped together in the F_{minmax} parameter. Each value of F_{minmax} produces a unique

value for density versus altitude (blue) line in Figure 4. Three values of F_{minmax} representing the average and two extremes are plotted. One attempt to provide a more realistic density profile that models the latitudinal effects for the particular arrival epoch and target inclination of the reference mission was to make the F_{minmax} parameter a dynamic function of the latitude. This function is not used for any of the trajectories covered by this preliminary analysis, and will not be discussed further in this paper.

Figure 4: Full range of Density versus Altitude from TitanGRAM

Spacecraft/Ballute Parameters

Parameter	Value
Mass: Ballute + S/C	500 kg
Mass: Ballute (Δ Mass)	42.4 kg
C_D : Ballute + S/C	1.37
C_D : S/C (after separation)	1.1
Area: Ballute + S/C	750 m ²
Area: S/C (after separation)	3 m ²

Separation Algorithm

In order to separate the ballute from the spacecraft at the proper time, a measurable observable is required. In the ideal case where the drag of the spacecraft is negligible compared to the ballute, it would be sufficient to integrate the deceleration measured by on-board accelerometers and release the ballute when sufficient delta-V had been achieved. As noted earlier, the entry speed is

very well known, so all that is needed to achieve a desired apoapsis altitude is to leave the atmosphere with a particular velocity. Unfortunately, as the nominal trajectory is targeted deeper in the atmosphere to accommodate navigation and atmospheric uncertainties, the drag on the spacecraft after ballute release can become significant. In order to minimize the propellant required to achieve the desired science orbit, another observation is required to modify the separation time to account for the drag effects after the ballute is released. Preliminary studies of Mars Aerocapture using ballutes showed that the maximum deceleration always occurred before the optimum separation time, so the maximum deceleration has been used to adjust the amount of integrated deceleration (delta-V from the ballute) that triggers release of the ballute. For the preliminary characterization of the ballute performance described below, the following very simple separation algorithm was used: "Release the ballute when the integrated delta-V achieves a value that depends on the observed maximum deceleration." This strategy depends on a "smooth" atmosphere to avoid spurious peaks due to transient fluctuations in the atmosphere that would produce spikes in the maximum deceleration. Smoothing would be required for this strategy to work with a realistic "noisy" atmosphere.

The following procedure was used to generate a unique value for the "integrated delta-V at separation" as a function of the maximum observed deceleration. Three entry states representing the highest, nominal, and lowest periapsis radii were picked from the 2000 dispersed entry states. For each of these three entry states, numerous trajectories were run using the full range of F_{minmax} values between [-1 and +1], where F_{minmax} was a particular value for each run. For each F_{minmax} -Entry State combination, a search was performed to find the optimum release time, such that the osculating value of the apoapsis altitude exactly achieved the desired value of 1700 km. Figure 5 shows the integrated deceleration (i.e. the cumulative Delta-V due to drag as measured by integrating the accelerometer output) versus the Instantaneous Deceleration (measured by the accelerometers) for the Nominal and 4 Extreme combinations of Entry State & F_{minmax} . The maximum observed deceleration and the integrated delta-V (i.e. the integrated accelerometer output) at the optimum release time were recorded for these 5 example trajectories, as well as for hundreds of other combinations of entry state and F_{minmax} and then plotted in Figure 6.

The 5 trajectories represented on Figure 5 all enter the atmosphere with zero measureable deceleration, and zero integrated "delta-V". The integrated accelerometer measurement (y-axis) increases monotonically with time, while the instantaneous deceleration reaches a peak and then decreases. The peak deceleration is smallest for $F_{minmax} = -1$ (i.e. for the thinnest atmosphere) and is a maximum for $F_{minmax} = +1$ (i.e. the thickest atmosphere). The pale-green "x" tics are for a Nominal State with an $F_{minmax} = -1$. The dark-green "+" tics are for a Nominal State with an $F_{minmax} = +1$. The three curves clustered in the middle all use a nominal $F_{minmax} = 0$, but use different periapsis altitudes: the blue "Δ"

are for the highest periapsis altitude (shallowest Flight Path Angle at entry), the black “•” mark the nominal periapsis altitude, while the red “V” represent the lowest periapsis altitude (steepest Flight Path Angle at entry). Higher altitude trajectories have similar effects as thinner atmospheric profiles.

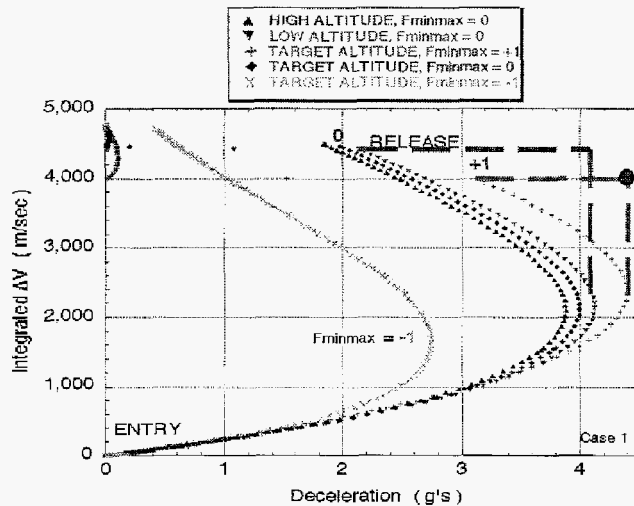


Figure 5: Integrated Deceleration (Delta-V) versus Instantaneous Deceleration for the Nominal and 4 Extreme combinations of Entry State & Fminmax.

Case 1: Target Accommodates $F_{minmax} = \pm 1$

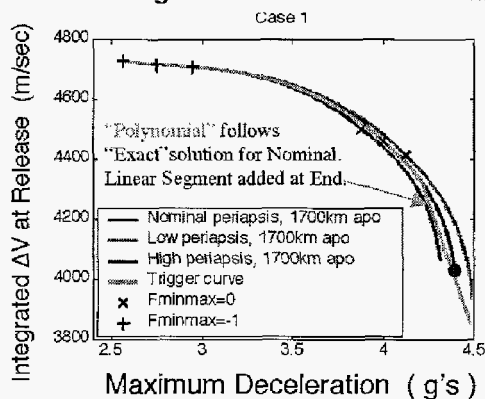


Figure 6: Integrated Deceleration (ΔV) at the Optimum Release Time versus Maximum Observed Deceleration for Three Entry States and the Full Range of $F_{minmax} [\pm 1]$

Figure 6 shows the maximum observed deceleration (x-axis) versus the integrated delta-V (i.e. the integrated accelerometer output) at the optimum release time (y-axis) for hundreds of F_{minmax} values for each of the 3 entry states (highest altitude periapsis, nominal target, and lowest altitude periapsis). The highest and lowest altitude results “bound” the possible solutions for all 2000 dispersed entry states. An “X” marks the $F_{minmax} = 0$ runs (near the center), while a “+” marks the lowest value of $F_{minmax} = -1$. The largest value of $F_{minmax} = +1$ at the highest deceleration is at the rightmost end of each “line of constant entry state”. Our original plan was to create an 8th order polynomial for

“integrated delta-V” as a function of the maximum deceleration and use it to trigger the ballute release in a Monte Carlo simulation of the dispersed entry states and sampled atmosphere models. The curvature at the highest values of F_{minmax} (highest decelerations) was such that a polynomial provided a poor fit, so the polynomial was only fit to the nominal values with decelerations less than 4.2 g’s. A linear fit of the last valid point from the polynomial and the $F_{minmax} = +1$ point defined the integrated delta-V at separation for decelerations higher than 4.2 g’s. The resulting separation “Polynomial” is plotted using the pale-green points in Figure 6. Before evaluating the performance of this very simple separation algorithm, some of the characteristics of the nominal and extreme cases will be discussed.

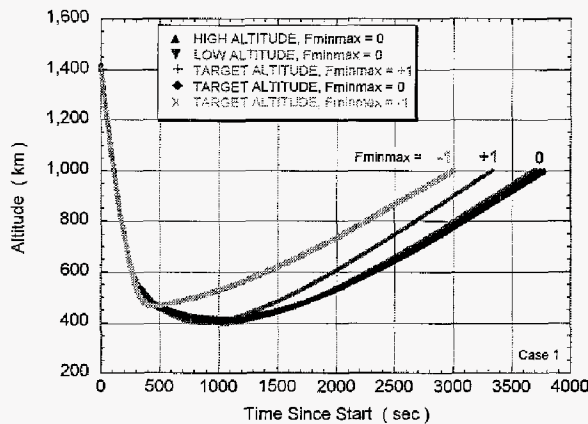


Figure 7: Instantaneous Altitude versus Time

Figure 7 shows the altitude history for the nominal and the 4 extreme cases. Although the nominal state enters the atmosphere with an osculating periapsis altitude of 469 km, drag prior to periapsis has the effect of lowering the actual minimum altitude to just above 400 km for most of the trajectories. If there were no atmosphere, periapsis would occur 407 seconds from the start of the simulation. The trajectory using the minimum density, $F_{minmax} = -1$ is noticeably different from the others. The thin atmosphere means that most of the drag occurs near periapsis, where drag has the least effect on the periapsis altitude. (For example, an impulsive “velocity reduction” at periapsis will lower apoapsis while having no effect on periapsis.) For the highest density trajectory ($F_{minmax} = +1$), a significant amount of deceleration occurs earlier in the trajectory, which has the effect of making the actual lowest altitude noticeably less than the osculating periapsis altitude at entry.

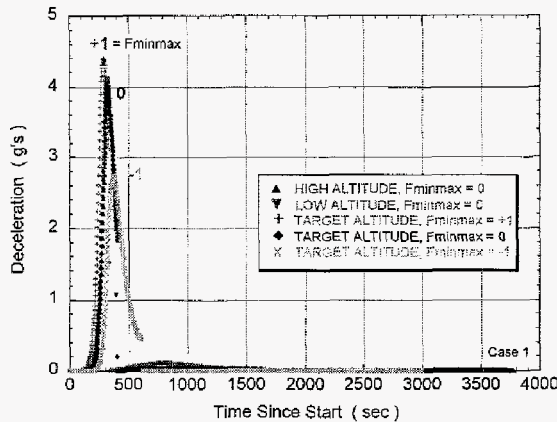


Figure 8: Instantaneous Deceleration versus Time

Figure 8 shows the total instantaneous deceleration versus the time since the start of the simulation. The thinnest atmosphere ($F_{minmax} = -1$) has the lowest peak deceleration, and holds on to the ballute the longest – to achieve the same integrated ΔV . For the densest atmosphere ($F_{minmax} = +1$), there is a small, but noticeable deceleration after the ballute was released, near the lowest altitude point on the trajectory.

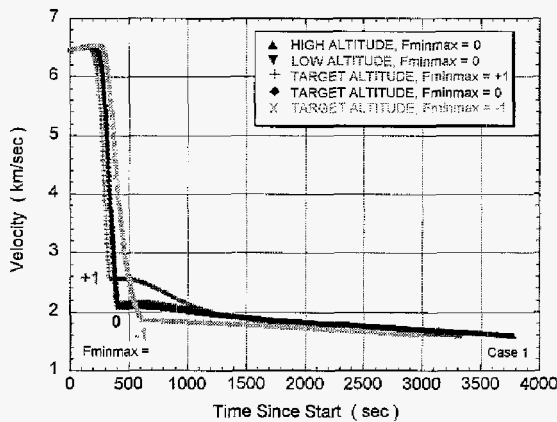


Figure 9: Instantaneous Velocity versus Time

Figure 9 shows the instantaneous, inertial velocity versus the time since the start of the simulation. The sudden change in the slope occurs when the ballute is released, and the deceleration drops suddenly. The slope beyond the 1500 second point is simply the gravitational effect associated with the increasing altitude. For the highest density case ($F_{minmax} = +1$), there is a significant velocity decrease between release and 1200 seconds that is caused by drag acting on the spacecraft body alone.

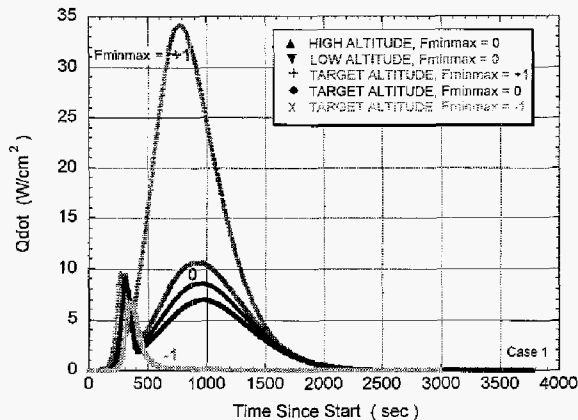


Figure 10: Instantaneous “Qdot” versus Time

Figure 10 shows the “free stream” heat flux, $Q_{dot} = 0.5 \cdot \text{density} \cdot \text{velocity}^3$. This parameter, when used with heat transfer coefficients that account for the effect of the flow field and surface accommodation, is useful for computing the temperature of the surface. The flow field is computed by our team members at NASA Langley, while the temperatures of various components are computed by our team members at Ball Aerospace in Boulder Colorado. The most interesting aspect of Figure 10 is for the densest atmosphere ($F_{minmax} = +1$) where the largest heating spike occurs after the ballute has been released. For the nominal atmosphere ($F_{minmax} = 0$), there is a noticeable second peak that is approximately equal to the first peak. For the four trajectories with a second peak, the ballute is released well before the lowest point in the trajectory, so the exponential density increase associated with the still decreasing altitude is enough to create a second peak. For the thinnest atmosphere ($F_{minmax} = -1$), the ballute is not released until after periapsis, so there is no opportunity for a second peak near the lowest altitude point.

This second peak is primarily due to the fact that this preliminary analysis targeted the approach hyperbola for the nominal entry state low enough to accommodate the largest imaginable dispersion for the atmospheric uncertainty. The developer of the TitanGRAM model, Jere Justus¹⁰, believes that data from the Cassini mission to Saturn will reduce the F_{minmax} uncertainty to a more manageable range of about $[\pm 0.23]$. The following discussion shows that reducing the F_{minmax} range to $[\pm 0.6]$ reduces the post aerocapture delta-V dispersion considerably.

Monte Carlo Results:

The previous discussion of Figure 6 described a “polynomial” separation algorithm where the integrated delta-V (i.e. the integrated accelerometer output) that triggered ballute release was a function of the maximum observed deceleration. The ballute is released when the integrated accelerometer measurement reaches the value that is determined by the maximum deceleration

for that particular trajectory. Inspection of Figure 6 shows that the algorithm should work very well for lower values of maximum deceleration (corresponding to lower values of F_{minmax}), because the maximum and minimum entry state curves result in nearly the same value. On the other hand, the algorithm will have difficulty at higher values of maximum deceleration (corresponding to higher densities for the higher values of F_{minmax}), because the optimum integrated delta-V at separation is significantly larger for the lower hyperbolic periapsis altitude (steeper FPA at entry) trajectories than for the higher altitude (shallower FPA) trajectories at a given maximum deceleration. The only way to reduce the targeting errors for large values of F_{minmax} would be to try to update the estimate of the entry state on the fly – and even that would not help to accommodate unpredictable atmospheric effects that occurred after separation.

To evaluate the effectiveness of the “Polynomial” separation algorithm, a Monte Carlo analysis was performed using a random sampling of the 2001 retargeted “knowledge” entry states, and a uniform sampling of 201 atmospheric profiles (i.e. 201 uniformly spaced values of F_{minmax}). Performance was characterized by evaluating the osculating apoapsis altitude at atmospheric exit and by computing the propulsive delta-V required to circularize at the 1700 km target altitude.

Figure 11 shows the results of the 2001 trajectory Monte Carlo study for two cases. The cumulative distribution fraction is plotted on the vertical axis, while the apoapsis altitude at atmospheric exit is plotted on the horizontal axis. The blue curve labeled “Case 1” was targeted low enough in the atmosphere to guarantee that the entry trajectory with the highest periapsis altitude would barely achieve the desired apoapsis altitude of 1700 km when the thinnest ($F_{minmax} = -1$) atmosphere was used. The red curve labelled “Case 3” was targeted to a higher altitude (shallower FPA at entry) where the entry trajectory with the second highest periapsis altitude would barely achieve 1700 km when F_{minmax} was -0.6 . For Case 3, the range of F_{minmax} sampled during the Monte Carlo was limited to ± 0.6 to represent better atmospheric knowledge. (Case 2 was so close to Case 1 that it is not discussed.) Since the nominal entry state for Case 3 has a higher periapsis altitude, the 2000 dispersed states were all adjusted to simulate the same dispersion about the nominal. The “Polynomial” that triggered separation for Case 1 is the one shown in Figure 6. Although not shown here, the Polynomial that triggered separation for Case 3 was derived in the same way, by first finding the exact solution for the nominal, highest and lowest altitude entry states for the range of F_{minmax} of interest, and then fitting a polynomial to the nominal values. The extreme entry states provided values at higher and lower maximum decelerations.

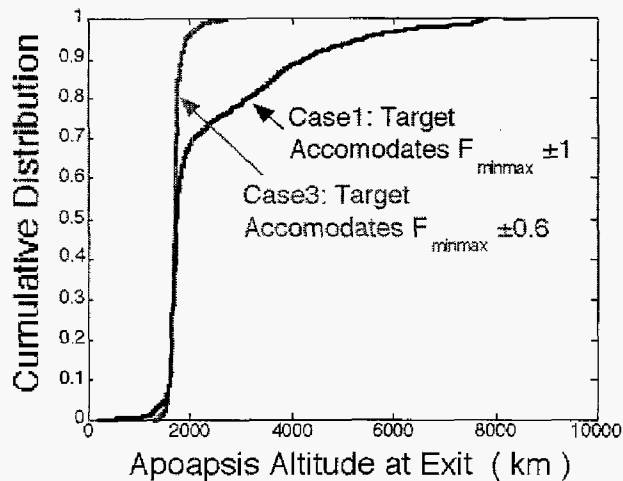


Figure 11: Monte Carlo results for Two Cases.

Figure 11 shows that this simple separation algorithm provides a workable solution for the largest imaginable atmospheric uncertainty, and provides a very accurate solution when more realistic atmospheric uncertainties are used. Since the post-Cassini dispersion in F_{minmax} is believed to be only ± 0.23 , the excellent Case 3 results for $F_{minmax} = \pm 0.6$ suggest that excellent ballute separation performance at Titan is possible.

The simple algorithm will not work as well when the atmospheric profile contains noise, which was not modeled in these preliminary cases, however, it may be possible to filter the measurement of the maximum deceleration and still find a workable solution for noisy atmospheric profiles. Similarly, all separation algorithms will suffer degraded performance if the atmospheric structure is significantly different than the modeled value when separation occurs early because the drag after separation will diverge from the expected value.

One aspect of the separation which seemed counter-intuitive is that when the entry state periapsis altitude is higher than the nominal, (i.e. the entry FPA is shallower than the nominal), the resulting apoapsis altitude will be below the target altitude. Similarly, entry state periapsis altitude is lower than the nominal, (i.e. the entry FPA is steeper than the nominal), the resulting apoapsis altitude will be higher than the target altitude. Since more drag is available for a steeper entry, why is a steeper entry more likely to remove less energy during the drag pass? Inspection of Figure 6 shows that for a given maximum deceleration that triggers separation, lower entry periapses (steeper FPA) require more delta-V reduction by the time of separation than higher entry periapses. By using the nominal entry state to determine the separation polynomial, the polynomial will trigger release before enough delta-V has been removed for the low altitude (steeper entry) cases so the apoapsis altitude at exit will be too high. Similarly, the polynomial will trigger release after too much delta-V has been removed for the high altitude (shallower entry) cases so the apoapsis altitude at exit will be too low. Since the high and low periapsis altitude at entry curves (in Figure 6)

only diverge when the deceleration is high, this effect is most noticeable for large values of F_{minmax} , where the ballute is released relatively early. When the deceleration is low (i.e. F_{minmax} is low), all of the curves are very close to the polynomial, so separation performance is much better.

Another way to quantify the separation performance is to compute the delta-V required to transfer from the exit orbit to the specified mapping orbit. For a 1700 km circular mapping orbit at Titan, a perfect ballute aerocapture with an osculating apoapsis at exit equal to 1700 km would require a propulsive maneuver of about 130 m/s at apoapsis to raise periapsis up to 1700 km. A second maneuver would be required to adjust any errors in the initial apoapsis value. The entry states and atmospheric dispersions can be characterized by a two parameter space: the osculating periapsis altitude at entry and F_{minmax} . Approximately 28 entry states that span the range of dispersed entry states at equal intervals were used with each of 30 values that spanned the F_{minmax} space to create a "grid" of results for both Case 1 and Case 3. The total delta-V to achieve a 1700 km was computed for each {altitude, F_{minmax} } pair and plotted in Figures 12 and 13.

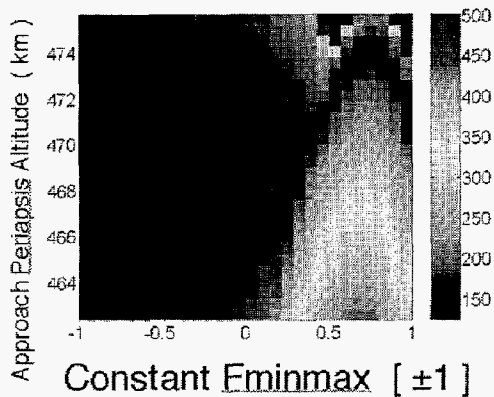


Figure 12: Case 1: Total Delta-V to Achieve 1700 km Circular Orbit

Figure 12 shows the results for Case 1. The nominal entry state has an osculating periapsis altitude at entry of 469 km. Smaller values of F_{minmax} correspond to the lower maximum deceleration trajectories, where all cases have similar optimum separation parameters so the propulsive delta-V is uniformly low. The black grid points in the upper right corner of Figure 12 correspond to trajectories that did not make it out of the atmosphere, because the ballute was not released soon enough, for the reasons that were already discussed (for high altitude entry states). The "black" color represents the fact that the delta-V required to overcome the excess drag in order to achieve the desired mapping orbit was not computed. The red & yellow region in the lower right corner of Figure 12 represents the low periapsis altitude, high deceleration cases where the ballute was released too soon, and significant propulsive delta-V was required to lower the apoapsis altitude during the transition phase following atmospheric exit. The effects of increasing the value of F_{minmax} can be best

understood by examining a single altitude, say 466 km. The delta-V is small for $F_{minmax} < 0.4$, then it increases to a maximum near F_{minmax} of about 0.7. Something unusual happens at very high values of F_{minmax} , because the delta-V decreases as F_{minmax} continues to increase from 0.7 to +1.0. Inspection of the "Polynomial" in Figure 6 shows that this unusual effect is an artifact from our use of a linear segment for the very high values of F_{minmax} . The line agrees with the nominal value at both ends (for $F_{minmax} \approx +0.4$ and +1.0) and is farthest from the nominal in between. Since the linear segment is below the nominal delta-V at separation, most entry states will trigger an early ballute release which results in a larger value of apoapsis altitude and a larger total delta-V to reach the target mapping orbit.

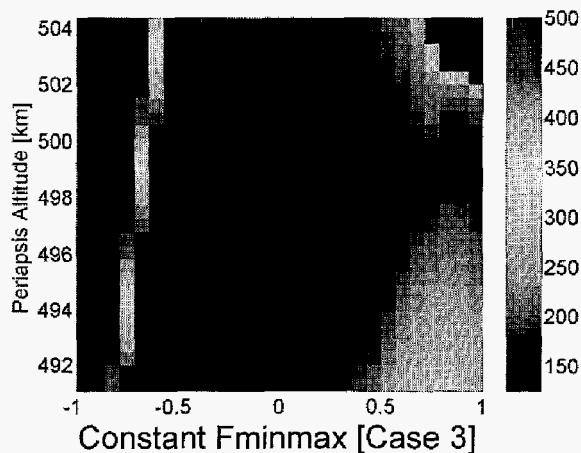


Figure 13: Case 3: Total Delta-V to Achieve 1700 km Circular Orbit

Figure 13 shows the results for Case 3. The nominal entry state has an osculating periapsis altitude at entry of 498 km. The higher nominal altitude was possible because the trajectory was designed to guarantee that the target apoapsis could be achieved for $F_{minmax} = -0.6$ (rather than -1.0 for Case 1). Note that the propulsive delta-V is uniformly low for all values of F_{minmax} in the target range of ± 0.6 . Delta-V values have been included for $F_{minmax} > +0.6$ to show that the algorithm performs quite well even when the atmospheric density is greater than the design requires. Delta-V values have also been included for $F_{minmax} < -0.6$ to show the downside of targeting to a higher altitude. If the atmospheric density is significantly thinner than the thinnest design value, there may be insufficient drag to capture into orbit. The black region at the left side of the plot shows the region where the total delta-V was not computed because the exit orbit was hyperbolic. The rainbow band shows that entry states with a lower osculating periapsis altitude at entry can accommodate a thinner atmosphere than those with a higher periapsis.

Comparing Figure 13 to Figure 12, it is immediately obvious that targeting to a higher periapsis altitude at entry results in lower total delta-V, for the larger values of F_{minmax} . Unfortunately, higher periapsis targets are less robust if the

atmosphere is significantly less dense than predicted. The arrival target will depend on the uncertainties in the navigation accuracy and the atmosphere models at the time of arrival. Larger uncertainties can be accommodated by targeting deeper in the atmosphere, but will result in a higher probability that a larger propulsive delta-V will be required to achieve the target orbit.

Separation Timing Errors:

The previous figures have shown the performance of a very simple separation algorithm, where the ballute is released as soon as the separation criterion is achieved. Because the release is a mechanism, there will be some difference between the actual release time and the commanded release time. Figure 14 shows the effect of release time errors on the apoapsis altitude at exit and the delta-V required to adjust the apoapsis altitude. Figure 14 was generated by computing the separation using the Polynomial for the same entry states and F_{minmax} values that were used to generate the converged, exact values shown in Figure 6. Subtracting the exact separation time from the separation time for the polynomial, and subtracting the exact apoapsis altitude (1700 km) from the apoapsis altitude for the polynomial results in the plot of apoapsis altitude error versus separation timing error shown in Figure 14.

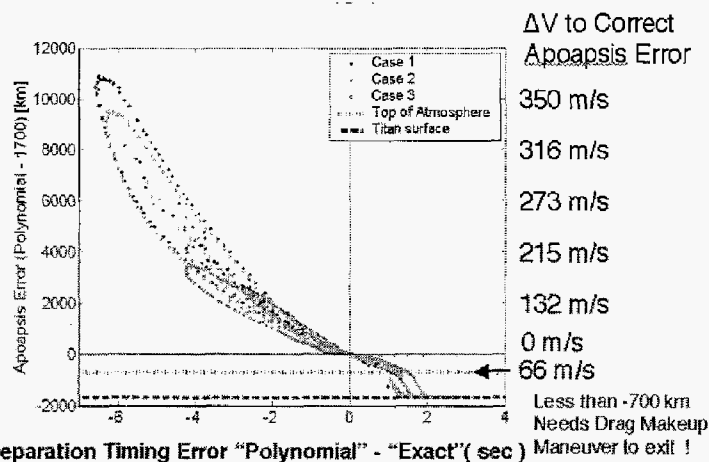


Figure 14: Effect of Timing Errors

The large "loops" that occur when separation occurs several seconds early are due to the linear segment of the "Polynomial" at the high deceleration region. For a nominal entry state, both ends of the linear segment give good release times, but the error is a maximum near the middle. The early release time means that not enough energy is removed, so apoapsis is too high. When the entry state is higher than the nominal, the polynomial results in a late separation where too much energy is removed from the trajectory. If separation is delayed by more than about 1 second, the orbit will not exit the atmosphere without immediate propulsive assistance! (The top of the atmosphere was defined to be 1000 km for this study.) The delta-V to correct the apoapsis altitude was computed assuming a 500 km periapsis altitude and noted at the

right side of Figure 14. Only 66 m/s is required to raise apoapsis from 1000 km to 1700 km. Unfortunately, the effects of drag will accumulate very rapidly if apoapsis is allowed to drop below 1000 km, so the delta-V cost cannot be extrapolated for those points where apoapsis is below 1000 km. It would be possible and probably prudent to design and fly an algorithm that would propulsively raise apoapsis if it ever dropped below 1000 km, but such an algorithm would be more complicated than the simple separation algorithm described above. On the other hand, separating early does not require such an algorithm. Separating many seconds earlier results in higher osculating apoapsis altitudes, which costs propellant to adjust, but it does not require propulsion while the spacecraft is in the atmosphere. Thus there is a tradeoff between flight software complexity, propellant mass, and risk that must be made based on the specific spacecraft and mission design.

Summary:

This paper discussed the current status of the trajectory related issues that factor into the overall ballute system design for aerocapture at Titan. This preliminary analysis was based on simplifying assumptions, such as constant drag coefficients and a nominal (smooth) atmosphere from TitanGRAM. The preliminary trajectories provided data for other team members to begin to size the ballute, evaluate the aerothermodynamic environment, develop separation algorithm concepts, and design an optimum system. Future work will include the effects of more realistic atmospheric effects on the candidate separation algorithms and will include the more realistic drag models from the preliminary aerothermodynamic analyses. Since this study is scheduled to span 3 years, we are only beginning to understand the issues associated with a ballute system. Updated results will be reported in future papers.

Acknowledgements:

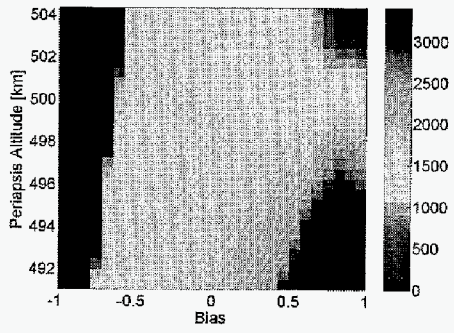
The work described was performed at the Jet Propulsion Laboratory (JPL), California Institute of Technology under contract with National Aeronautics and Space Administration (NASA). Funding for this study was provided by the NASA Office of Space Science. The authors would like to thank Bonnie James and Michelle Munk at the MSFC In Space Propulsion Program office for their sponsorship and excellent guidance in the management of these efforts.

References:

1. Angus McDonald, "A Light-Weight Inflatable Hypersonic Drag Device for Planetary Entry", Association Aeronautique de France Conf. at Arcachon, France, March 16-18, 1999.

2. Angus McRonald, "A Light-Weight Inflatable Hypersonic Drag Device for Venus Entry" AAS/AIAA Astrodynamics Specialist Conf., Girdwood, Alaska, Aug 16-19, 1999. AAS 99-355
3. Angus Mc Ronald, "A Light-Weight Hypersonic Inflatable Drag Device For a Neptune Orbiter", AAS/AIAA Space Flight Mechanics Meeting, Clearwater, FL, January 23-26, 2000. AAS 00-170
4. Jeffery L. Hall , "A Review of Ballute Technology for Planetary Aerocapture", 4th IAA Conference on Low Cost Planetary Missions, Laurel, MD, May 2-5, 2000.
5. Kevin Miller, "Gossamer Ballute Aerocapture Final Report". September 25, 2002. Contract #1205966.
6. Kevin Miller, Jake Lewis, Bill Trochman, Jim Stein, Daniel T. Lyons, Richard G. Wilmoth "Trailing Ballute Aerocapture: Concept and Feasibility Assessment",
7. Justus . Personal Communication. "TitanGRAM beta version on CD"
8. Rob Haw. Personal Communication. "2001 Knowledge and 2001 Delivery States based on the Titan Aeroshell Aerocapture Working Group reference mission".
9. Mary Kay Lockwood, "Titan Aeroshell Aerocapture Systems Analysis Review", August 29 & 30, 2002.
10. Jere Justus. Personal Communication. "Expected Post Cassini Atmospheric Modelling Improvements"

Case 3: Osculating apoapsis at atmospheric exit [km]



Total ΔV to achieve 1700 km (m/sec)

